Electronic Supplementary Material (ESI) for Journal of Materials Chemistry C.

Supporting Information

Effects of neutral point defects on the solid-state electrolyte Li_3ScBr_6

Ming Jiang[1], Zhi-Wen Chen[2,*], Adwitiya Rao[2], Li-Xin Chen[2], Parvin Adeli[3], Patrick Mercier[3], Yaser Abu-Lebdeh[3], Chandra Veer Singh[2,4,*]

[1]Institutes of Physical Science and Information Technology, Anhui University, Hefei 230601, China

[2]Department of Materials Science and Engineering, University of Toronto, Ontario M5S 3E4, Canada

[3]Energy, Mining, and Environment Research Centre, National Research Council of Canada, 1200 Montreal Road, Ottawa, Ontario K1A 0R6, Canada

[4]Department of Mechanical and Industrial Engineering, University of Toronto, Ontario M5S 3G8, Canada

Table S1. The lattice constant and band gap of Li_3ScBr_6 at different U_{eff} values.

U_{eff} (eV)	Lattice constant (Å)			band gap (eV)
	a	*b*	*c*	
0	6.77	11.73	6.69	2.97
1	6.77	11.74	6.69	3.11
2	6.78	11.75	6.71	3.26
3	6.79	11.76	6.72	3.66
4	6.79	11.76	6.72	3.69
5	6.79	11.77	6.72	3.72
6	6.79	11.76	6.75	3.77

Table S2. Defect formation energy of Li_3ScBr_6 at different U_{eff} values.

	U_{eff}=0	U_{eff}=1	U_{eff}=2	U_{eff}=3	U_{eff}=4	U_{eff}=5	U_{eff}=6
V_{Li}	2.50	2.51	2.50	2.50	2.48	2.48	2.47
V_{Sc}	7.65	7.64	7.64	7.64	7.64	7.62	7.63
V_{Br}	2.92	2.91	2.94	2.94	2.94	2.93	2.96
Li_{int}	0.49	0.49	0.50	0.52	0.47	0.53	0.51
Sc_{int}	2.83	2.79	2.78	2.78	2.78	2.78	2.76
Br_{int}	1.19	1.18	1.18	1.19	1.16	1.17	1.17
Li_{Sc}	4.40	4.37	4.41	4.42	4.39	4.41	4.41
Li_{Br}	2.76	2.73	2.75	2.76	2.77	2.74	2.72
Sc_{Li}	1.77	1.80	1.81	1.81	1.76	1.75	1.78
Sc_{Br}	5.94	5.91	5.92	5.91	5.90	5.90	5.92
Br_{Li}	3.26	3.28	3.29	3.26	3.25	3.26	3.24
Br_{Sc}	7.34	7.34	7.36	7.39	7.37	7.39	7.36

Table S3. Li^+ ionic conductivity (σ) and activation energy (E_a) of pristine Li_3ScBr_6 at different U_{eff} values.

	σ (mS/cm)	E_a (eV)
U_{eff}=0	1.36	0.221
U_{eff} =1	1.34	0.219
U_{eff} =2	1.37	0.218
U_{eff} =3	1.39	0.216
U_{eff} =4	1.38	0.216
U_{eff} =5	1.42	0.215
U_{eff} =6	1.38	0.217

Table S4. Formation energy (eV) of point defects in Li_3ScBr_6 at different defect concentrations. V_X: X vacancy; X_{int}: X interstitial; X_Y: X occupying the Y lattice site (X, Y = Li, Sc or Br)

	0.625%	1.25%	1.875%	2.50%	3.125%
V_{Li}	2.42	2.50	2.61	2.69	2.73
V_{Sc}	7.58	7.64	7.61	7.68	7.71
V_{Br}	2.86	2.94	2.98	2.95	3.01
Li_{int}	0.55	0.52	0.6	0.64	0.65
Sc_{int}	2.67	2.78	2.88	2.94	2.92
Br_{int}	1.23	1.19	1.22	1.26	1.28
Li_{Sc}	4.36	4.42	4.44	4.30	4.38
Li_{Br}	2.66	2.76	2.72	2.87	2.83
Sc_{Li}	1.72	1.81	1.83	1.89	1.95
Sc_{Br}	5.82	5.91	5.96	6.03	6.10
Br_{Li}	3.17	3.26	3.3	3.38	3.45
Br_{Sc}	7.20	7.39	7.41	7.35	7.48

Table S5. Bulk modulus (GPa) of defective Li_3ScBr_6 at different defect concentrations. V_X: X vacancy; X_{int}: X interstitial; X_Y: X occupying the Y lattice site (X, Y = Li, Sc or Br).

	0.625%	1.25%	1.875%	2.50%	3.125%
V_{Li}	14.32	13.66	13.25	12.41	12.01
V_{Sc}	7.57	6.70	6.02	5.42	4.06
V_{Br}	14.12	13.78	12.09	11.48	10.95
Li_{int}	14.71	13.26	12.88	11.91	10.43
Br_{int}	16.25	15.53	13.37	12.5	11.45
Li_{Sc}	11.95	10.69	9.35	8.44	8.30
Sc_{Br}	14.69	12.23	11.41	10.40	9.35
Br_{Li}	9.77	6.88	6.15	5.58	4.19
Br_{Sc}	11.61	10.91	9.84	8.11	7.55

Table S6. Shear modulus (GPa) of defective Li_3ScBr_6 at different defect concentrations. V_X: X vacancy; X_{int}: X interstitial; X_Y: X occupying the Y lattice site (X, Y = Li, Sc or Br).

	0.625%	1.25%	1.875%	2.50%	3.125%
V_{Li}	9.86	7.27	6.69	5.02	4.15
V_{Sc}	10.9	8.72	7.09	6.51	5.17
V_{Br}	9.26	7.40	6.33	5.71	4.24
Li_{int}	11.01	10.66	9.04	8.89	7.23
Br_{int}	8.08	6.14	5.06	4.68	3.57
Li_{Sc}	10.12	9.29	8.18	7.41	6.79
Sc_{Br}	9.85	8.88	7.84	7.29	6.61
Br_{Li}	9.32	8.29	7.34	6.89	5.63
Br_{Sc}	9.21	8.68	7.81	6.27	5.34

Table S7. Young's modulus (GPa) of defective Li_3ScBr_6 at different defect concentrations. V_X: X vacancy; X_{int}: X interstitial; X_Y: X occupying the Y lattice site (X, Y = Li, Sc or Br).

	0.625%	1.25%	1.875%	2.50%	3.125%
V_{Li}	21.87	18.53	17.68	16.06	15.55
V_{Sc}	21.49	18.24	16.23	15.01	14.3
V_{Br}	20.18	18.82	18.32	17.47	15.16
Li_{int}	20.35	17.73	16.61	15.22	14.38
Br_{int}	19.91	16.27	15.59	14.16	13.02
Li_{Sc}	20.59	21.62	19.12	18.53	16.93
Sc_{Br}	22.75	21.41	20.9	19.71	18.79
Br_{Li}	19.76	17.74	15.75	14.89	13.15
Br_{Sc}	21.44	20.57	19.13	17.80	16.73

Table S8. Phase equilibria and minimum decomposition energies (ΔE_D: meV/atom) of ideal and defective Li_3ScBr_6 at the interface with $LiCoO_2$ cathode material. V_X: X vacancy; X_{int}: X interstitial; X_Y: X occupying the Y lattice site (X, Y = Li, Sc or Br).

C_{SSE}	$C_{electrode}$	x_m	Phase equilibria at x_m	ΔE_D
Pristine	$LiCoO_2$	0.38	CoO, LiBr, Br, Sc_2O_3	-93.16
	$Li_{0.5}CoO_2$	0.34	CoO, LiBr, Br, Sc_2O_3	-100.53
V_{Li}	$LiCoO_2$	0.38	CoO, LiBr, Br, Sc_2O_3	-93.89
	$Li_{0.5}CoO_2$	0.35	CoO, LiBr, Br, Sc_2O_3	-101.36
V_{Sc}	$LiCoO_2$	0.35	CoO, LiBr, Br, Sc_2O_3	-86.23
	$Li_{0.5}CoO_2$	0.32	CoO, LiBr, Br, Sc_2O_3	-92.71
V_{Br}	$LiCoO_2$	0.38	CoO, LiBr, Br, Sc_2O_3	-111.41
	$Li_{0.5}CoO_2$	0.35	CoO, LiBr, Br, Sc_2O_3	-119.75
Li_{int}	$LiCoO_2$	0.37	CoO, LiBr, Br, Sc_2O_3	-109.68
	$Li_{0.5}CoO_2$	0.34	CoO, LiBr, Br, Sc_2O_3	-117.80
Br_{int}	$LiCoO_2$	0.37	CoO, LiBr, Br, Sc_2O_3	-92.44
	$Li_{0.5}CoO_2$	0.34	CoO, LiBr, Br, Sc_2O_3	-99.71
Li_{Sc}	$LiCoO_2$	0.34	CoO, LiBr, Br, Sc_2O_3	-85.52
	$Li_{0.5}CoO_2$	0.31	CoO, LiBr, Br, Sc_2O_3	-91.92
Sc_{Br}	$LiCoO_2$	0.18	CoO, LiBr, Br, Sc_2O_3	-170.74
	$Li_{0.5}CoO_2$	0.37	CoO, LiBr, Br, Sc_2O_3	-179.49
Br_{Li}	$LiCoO_2$	0.38	CoO, LiBr, Br, Sc_2O_3	-90.76
	$Li_{0.5}CoO_2$	0.34	CoO, LiBr, Br, Sc_2O_3	-97.35
Br_{Sc}	$LiCoO_2$	0.34	CoO, LiBr, Br, Sc_2O_3	-88.37
	$Li_{0.5}CoO_2$	0.31	CoO, LiBr, Br, Sc_2O_3	-96.25

Table S9. Phase equilibria and minimum decomposition energies (ΔE_D: meV/atom) of ideal and defective Li_3ScBr_6 at the interface with $LiFePO_4$ cathode material. V_X: X vacancy; X_{int}: X interstitial; X_Y: X occupying the Y lattice site (X, Y = Li, Sc or Br).

C_{SSE}	$C_{electrode}$	x_m	Phase equilibria at x_m	ΔE_D
Pristine	$LiFePO_4$	0.68	LiBr, $ScPO_4$, $Fe_3(PO_4)_2$	-12.73
	$FePO_4$	0.38	LiBr, $LiFeBr_4$, $ScPO_4$	-58.19
V_{Li}	$LiFePO_4$	0.66	$LiFeBr_4$, $ScPO_4$, $Fe_3(PO_4)_2$, LiBr	-14.92
	$FePO_4$	0.38	Br, $ScPO_4$, LiBr, $LiFeBr_4$	-58.65
V_{Sc}	$LiFePO_4$	0.21	$ScPO_4$, $ScBr_3$, $LiFeBr_4$, LiBr	-21.43
	$FePO_4$	0.44	Br, $Li_3Sc_2(PO_4)_3$, LiBr, $LiFeBr_4$	-54.45
V_{Br}	$LiFePO_4$	0.02	Fe_2P, ScBrO, $ScPO_4$, $ScBr_3$, LiBr	-20.64
	$FePO_4$	0.41	$LiFeBr_4$, LiBr, $LiFePO_4$, $ScPO_4$	-74.36
Li_{int}	$LiFePO_4$	0.02	LiBr, $ScPO_4$, Fe_2P, $ScBr_3$, ScBrO	-20.14
	$FePO_4$	0.40	$ScPO_4$, LiBr, $LiFePO_4$, $LiFeBr_4$	-73.25
Br_{int}	$LiFePO_4$	0.66	LiBr, $ScPO_4$, $Fe_3(PO_4)_2$, $LiFeBr_4$	-14.79
	$FePO_4$	0.47	$Li_3Sc_2(PO_4)_3$, $ScPO_4$, Br, $LiFeBr_4$	-57.75
Li_{Sc}	$LiFePO_4$	0.60	$ScPO_4$, $LiFeBr_4$, $Fe_3(PO_4)_2$, LiBr	-17.09
	$FePO_4$	0.44	Br, LiBr, $LiFeBr_4$, $Li_3Sc_2(PO_4)_3$	-54.07
Sc_{Br}	$LiFePO_4$	0.05	LiBr, Fe_2P, ScBrO, $ScBr_3$, FeP	-78.60
	$FePO_4$	0.47	LiBr, $Fe_3(PO4)_2$, $ScPO_4$, $LiFeBr_4$	-116.19
Br_{Li}	$LiFePO_4$	0.64	$Fe_3(PO_4)_2$, $LiFeBr_4$, LiBr, $ScPO_4$	-17.25
	$FePO_4$	0.38	$ScPO_4$, Br, LiBr, $LiFeBr_4$	-58.19
Br_{Sc}	$LiFePO_4$	0.26	$ScPO_4$, LiFeBr4, $ScBr_3$, LiBr	-26.45
	$FePO_4$	0.44	LiBr, Br, $Li_3Sc_2(PO_4)_3$, $LiFeBr_4$	-54.07

Figure S1. Mean square displacement (MSD) of Li^+ ions in defective Li_3ScBr_6. V_X: X vacancy; X_{int}: X interstitial; X_Y: X occupying the Y lattice site (X, Y = Li, Sc or Br).

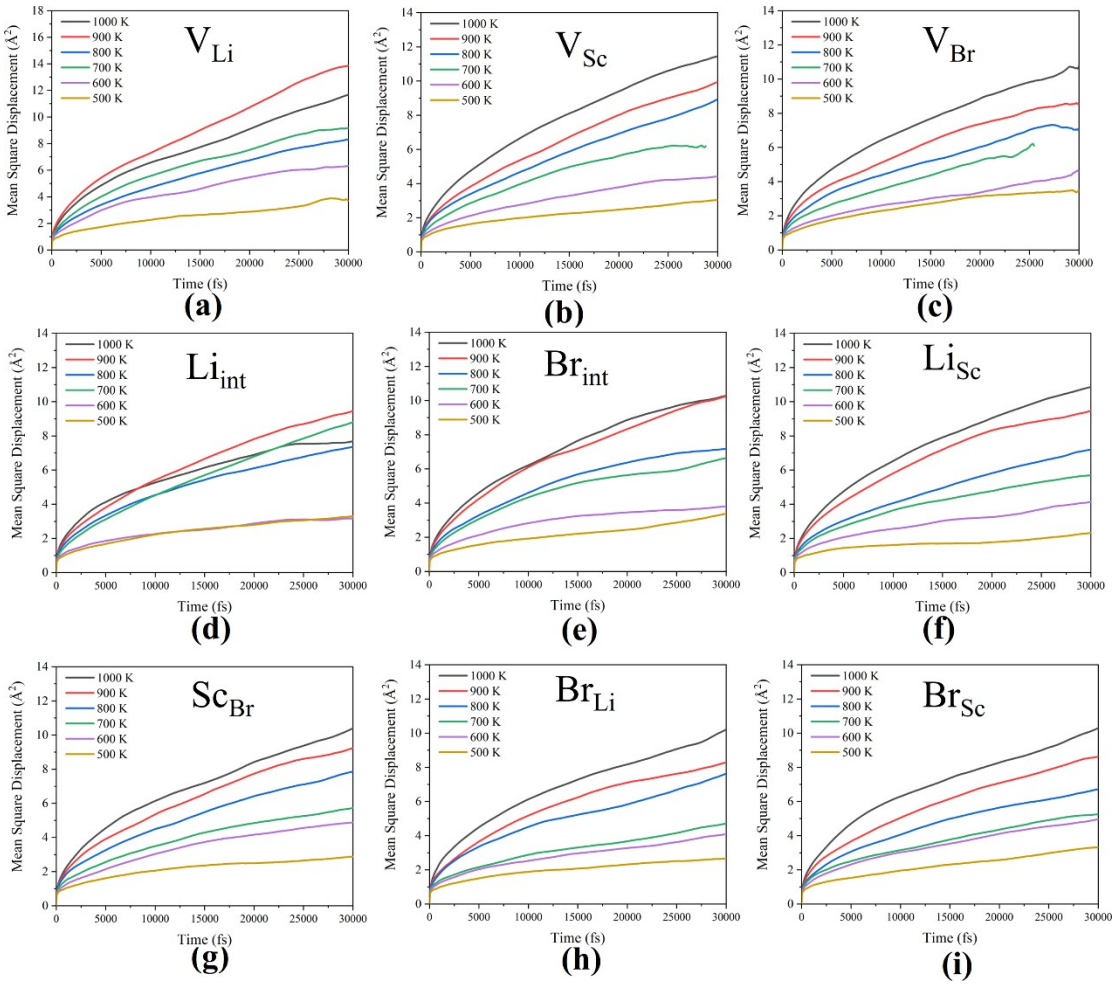

Figure S2. Arrhenius plot of the diffusion coefficient of defective Li_3ScBr_6. V_X: X vacancy; X_{int}: X interstitial; X_Y: X occupying the Y lattice site (X, Y = Li, Sc or Br).

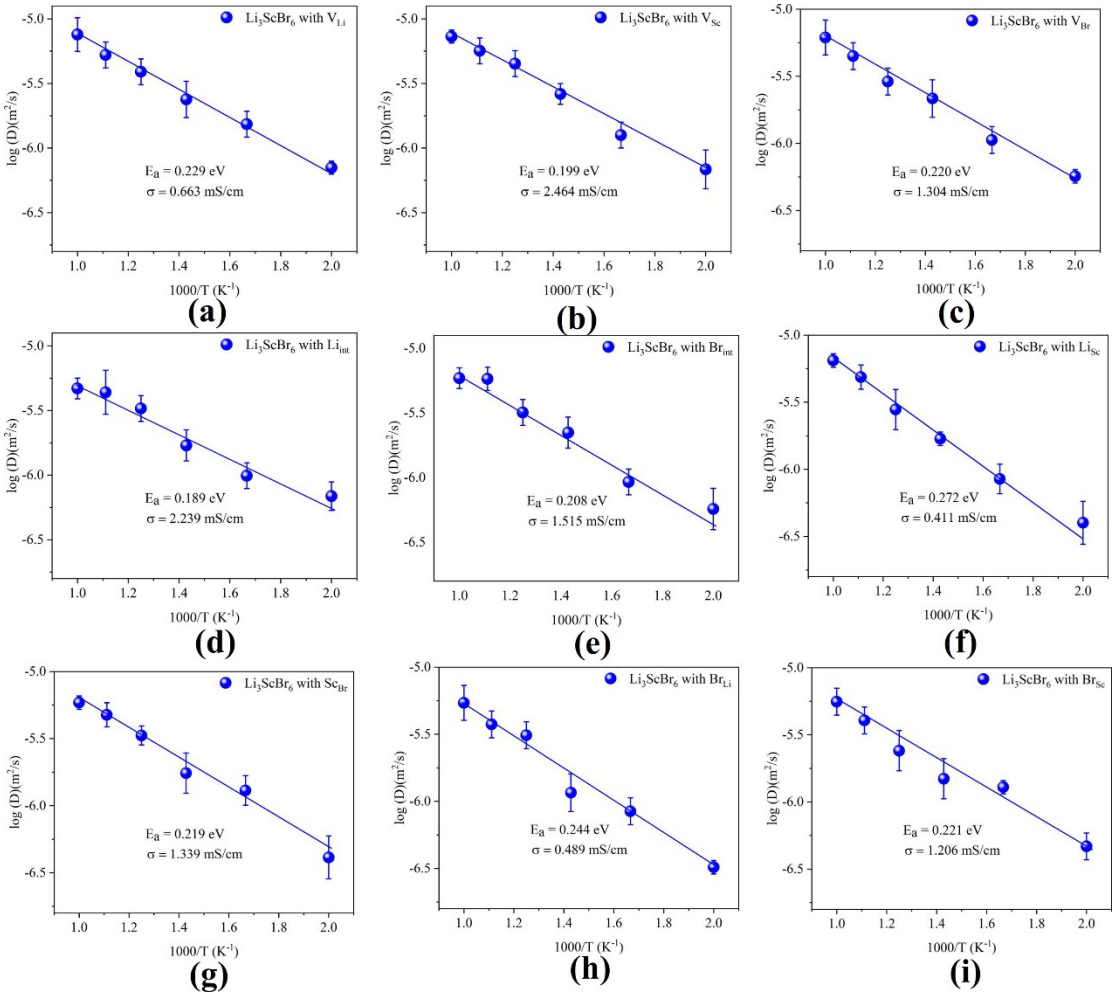

Figure S3. Diffusion path of Li^+ ions in defective Li_3ScBr_6. The yellow surface corresponds to the ionic conduction path, and the regions enclosed with blue surfaces correspond to the stable lithium-ion positions. V_X: X vacancy; X_{int}: X interstitial; X_Y: X occupying the Y lattice site (X, Y = Li, Sc or Br).